



**Michigan
Technological
University**

Michigan Technological University
Digital Commons @ Michigan Tech

Dissertations, Master's Theses and Master's Reports

2020

Radio Frequency Studies of Soot Loading and Ammonia Storage on a Diesel Particulate Filter with a SCR Catalyst Coating

Shreyans Sethia

Michigan Technological University, sssethia@mtu.edu


Copyright 2020 Shreyans Sethia

Recommended Citation

Sethia, Shreyans, "Radio Frequency Studies of Soot Loading and Ammonia Storage on a Diesel Particulate Filter with a SCR Catalyst Coating", Open Access Master's Report, Michigan Technological University, 2020.

<https://doi.org/10.37099/mtu.dc.etr/1085>

Follow this and additional works at: <https://digitalcommons.mtu.edu/etr>

 Part of the [Automotive Engineering Commons](#), [Chemical Engineering Commons](#), and the [Mechanical Engineering Commons](#)

**RADIO FREQUENCY STUDIES OF SOOT LOADING AND
AMMONIA STORAGE ON A DIESEL PARTICULATE FILTER
WITH A SCR CATALYST COATING**

By

Shreyans Sethia

A REPORT

Submitted in partial fulfillment of the requirements for the degree of

MASTER OF SCIENCE

In Mechanical Engineering

MICHIGAN TECHNOLOGICAL UNIVERSITY

2020

© 2020 Shreyans Sethia

This report has been approved in partial fulfillment of the requirements for the Degree of MASTER OF SCIENCE in Mechanical Engineering.

Department of Mechanical Engineering – Engineering Mechanics

Report Advisor: *Dr. Jeffrey Naber*
Committee Member: *Dr. Jason Blough*
Committee Member: *Dr. David Kubinski*
Department Chair: *Dr. William Predebon*

Table of Contents

| | |
|---|----|
| Radio Frequency Studies of Soot Loading and Ammonia Storage on a Diesel Particulate Filter with a SCR Catalyst Coating..... | 1 |
| List of figures..... | 3 |
| List of tables..... | 5 |
| Acknowledgements..... | 6 |
| List of abbreviations | 7 |
| Abstract..... | 8 |
| 1 Introduction..... | 9 |
| 2 Literature review | 12 |
| 2.1 Detection of the ammonia loading of a Cu Chabazite SCR catalyst by a radio frequency-based method..... | 12 |
| 2.2 Advanced RF Particulate Filter Sensing and Controls for Efficient After-treatment Management and Reduced Fuel Consumption | 12 |
| 3 Experimental Setup..... | 14 |
| 3.1 SDPF | 14 |
| 3.2 Test Phases | 14 |
| 3.2.1 Preparation Phase..... | 14 |
| 3.2.2 Testing phase | 15 |
| 3.3 Experiment Procedure | 16 |
| 3.4 Radio Frequency Spectrum | 17 |
| 3.5 Test Cases..... | 21 |
| 4 Results and Observations..... | 22 |
| 4.1 RF spectrum interaction with soot..... | 22 |
| 4.2 Temperature dependence of RF spectrum in presence of Soot..... | 23 |
| 4.3 RF spectrum interaction with ammonia | 25 |
| 4.4 Verification for running each test empty of any soot and ammonia from previous test..... | 29 |
| 4.5 Quantitative Analysis of soot loading and ammonia storage | 30 |
| 4.5.1 Quantitative measurement of soot loading at various temperatures | 30 |

| | | |
|-------|---|----|
| 4.5.2 | Quantitative analysis of ammonia's effect on the RF spectrum change under various soot loading condition. | 33 |
| 4.5.3 | Quantitative analysis for simultaneously calculating soot and ammonia loading at light soot loading cases. | 34 |
| 5 | Conclusion | 36 |
| 6 | References..... | 37 |

List of figures

| | |
|---|----|
| Figure 1: Preparation Phase Setup with SDPF | 15 |
| Figure 2: Heated Gas bench test setup..... | 16 |
| Figure 3: Interior and Exterior of the SDPF | 16 |
| Figure 4: Procedure for the test with respect to temperature profile | 17 |
| Figure 5: SDPF with RF antenna and TE111 Resonant EM wave | 18 |
| Figure 6: RF spectrum with various resonant peaks..... | 19 |
| Figure 7: Resonant modes inside SDPF..... | 20 |
| Figure 8: RF spectrum comparison for various soot loading cases at 228° C | 22 |
| Figure 9: temperature dependence of RF spectrum for 76% soot loading case..... | 23 |
| Figure 10: RF spectrum variation with respect to temperature for various soot loading cases. (A) RF spectrum change with respect to temperature for 0% soot loading case. (B) RF spectrum change with respect to temperature for 10% soot loading case. (C) RF spectrum change with respect to temperature for 40% soot loading case. (D) RF spectrum change with respect to temperature for 76% soot loading case..... | 24 |
| Figure 11: RF spectrum change under various ammonia loading condition at 0% soot loading..... | 25 |
| Figure 12: RF spectrum change under various ammonia loading condition at 2.8% soot loading..... | 26 |
| Figure 13: RF spectrum change under various ammonia loading condition at 7.8% soot loading..... | 26 |
| Figure 14: RF spectrum change under various ammonia loading condition at 10% soot loading..... | 27 |
| Figure 15: RF spectrum change under various ammonia loading condition at 22.6% soot loading..... | 27 |
| Figure 16: RF spectrum change under various ammonia loading condition at 76% soot loading..... | 28 |

| | |
|---|----|
| Figure 17: Validation for running each test empty of soot and ammonia in SDPF. (A) RF spectrum for various soot loading cases at 200° C when the SDPF was saturated with ammonia. (C) RF spectrum for various soot loading cases at 200° C after soot was burned and ammonia desorbed. | 29 |
| Figure 18: Verification that no soot was burned after RF spectrum temperature dependence analysis..... | 30 |
| Figure 19: Frequency domain selection for 76% soot loading case for quantitative measurement of soot loading at various temperatures..... | 31 |
| Figure 20: Mean amplitude of all soot loading cases at various temperature for the frequency domain selected..... | 32 |
| Figure 21: Quantitative model for estimating soot loading when mean amplitude and the instantaneous temperature is known | 32 |
| Figure 22: Quantitative analysis of ammonia's effect on the RF spectrum change under various soot loading condition and large frequency domain | 33 |
| Figure 23: Quantitative analysis of ammonia's effect on the RF spectrum change under various soot loading condition and small frequency domain..... | 34 |
| Figure 24: Quantitative analysis for simultaneously calculating soot and ammonia loading at light soot loading cases. (A) RF spectrum for all soot loading cases when no ammonia was stored in the SDPF. (B) 4 th Resonant peak of the four light soot loading cases when no ammonia was stored in the SDPF. (B) 4 th Resonant peak of the four light soot loading cases when the SDPF was empty and saturated with ammonia at the temperature of 226° C. (C) Mean amplitude of 4 th Resonant peak in the frequency domain selected when SDPF was empty and saturated with ammonia. (D) peak frequency of the 4 th resonant peak when the SDPF was empty and saturated of ammonia. | 35 |

List of tables

| | |
|--|----|
| Table 1: Experimental cases | 21 |
| Table 2: Constant parameters in preparation and testing phase..... | 21 |

Acknowledgements

I would like to acknowledge and thank everyone involved in this project in any manner. Firstly, I would like to thank Dr. David Kubinski who introduced me to RF sensing technologies and help me throughout the process to work towards my objectives and completion of the research. I would like to thank Dr. Jeffrey Naber for providing research funding, insights and invaluable discussion on this project. Dr. Naber's leadership has guided me throughout the research and motivated me to do my best quality work on this project. I would like to thank my team at Ford Motor Company for helping me in this process. Dr. Xin Liu for helping setup soot loading, Dr. David Bilby for showing various analytical procedures, Mr. Evangelos Skoures, Mr. Zaid Alnaqash and Dr. V.V. Zambare (Shekhar) for their invaluable support and inspiration. Last but not least Mr. Garlan Huberts for giving me the opportunity to work at Ford Motor Company and finally, Michigan Technological University to make me intellectually capable to tackle this project. Once again, I thank everyone involved who helped me in my endeavor.

List of abbreviations

DPF – Diesel particulate filter

SCR – selective catalyst reduction

SDPF – Selective diesel particulate filter

NO_x – Nitrogen oxides

NH₃ – Ammonia

RF – Radio frequency

CO₂ – Carbon dioxide

N₂ – Nitrogen

O₂ – Oxygen

H₂O – Water

NO – Nitrogen Oxide

NO₂ – Nitrogen dioxide

FTIR - Fourier-transform infrared spectroscopy

° C – Degree Celsius

TE – Transverse electric

ppm – part per million

Abstract

In the exhaust system of some diesel vehicles, the diesel particulate filter (DPF) is loaded with a selective catalyst reduction (SCR) wash coat. This combined catalyst, referred to as a SDPF, serves two functions by trapping soot and by reducing NO_x emissions. The latter is accomplished via reactions of NO_x with NH_3 stored on the SCR wash coat. The NH_3 is dosed, as urea, upstream of the SDPF.

The radio frequency (RF) measurement technique has been shown to be a viable method for measurement of the amount of soot loaded onto DPF's ^[1]. Additional studies have demonstrated the technique's utility in determining the amount of NH_3 stored on SCR catalysts ^[2]. In one configuration of the method, a microwave resonant cavity is formed by the metal can encasing the enclosed catalyst. Two metal probes acting as antennas are placed on either side of the catalyst. Power transmitted between the antennas is monitored as the frequency of the signal is swept. At certain frequencies, determined by the cavity's geometry and the dielectric properties of the catalyst, resonance is achieved. Measurements of the resonance frequencies, the signal amplitude at resonance, and the mean amplitude over a frequency range give information on the dielectric properties of the catalyst. These properties change upon soot and NH_3 loading.

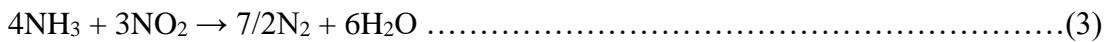
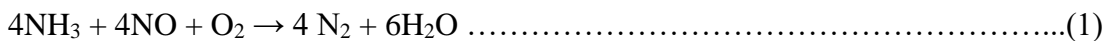
In this work we show how the RF response is influenced by both the soot and NH_3 loading on the SDPF. We demonstrate the comparative responses for each and show how the soot loading can be determined with little influence by the stored NH_3 . We also demonstrate how for the case of "light" soot loading, before the attenuation of the signal by the soot dominates the RF response, simultaneous measurements of both the soot loading and NH_3 storage can be achieved.

1 Introduction

In recent times, due to continuously increasing constraints to reduce the amount CO₂ released from vehicles, diesel engines are being preferred in the market for heavy-duty applications. To reduce all kinds of emissions from the engine, advanced after-treatment systems for exhaust are being developed. The conventional three-way catalyst is not enough to comply with the emission standards as it is for stoichiometric operations only and cannot reduce NO_x under the lean conditions at which diesel engine operate. To reduce the NO_x emissions, many modern diesel vehicles use the Selective Catalyst Reduction (SCR) system. For this, injected ammonia (NH₃) selectively reduces NO_x to N₂ and water [2] on the catalyst wash-coat under lean exhaust condition. The ammonia is injected as a urea solution upstream of the SCR catalyst which is then converted to ammonia on the SCR surface via a thermolysis and hydrolysis process.

Diesel vehicles also emit unwanted soot, which in modern vehicles is removed from the exhaust stream by the diesel particulate filter (DPF). The DPF removes the soot by a combination of filtration techniques [3]. This filtered particulate matter or as mentioned in this report, soot, is stored on the surface of the DPF and continuous or intermittent thermal regenerative processes are used to clean the DPF from this stored particulate matter. The DPF is very efficient in reducing the emission of diesel particle mass and number [5]. During engine operation soot particles are collected in the DPF, and as the loading of these particles continue they generate a high back pressure which leads to a performance loss of the engine. It is imperative that this back pressure is removed so that the appropriate working standard of the engine can be achieved, and the life of the engine is not reduced. Therefore, thermal regeneration processes are performed inside the DPF, the stored soot is oxidized with the help of oxygen or NO₂. This regeneration is typically triggered by the pressure differential measurement across the DPF.

SCR is deployed in after-treatment system to convert NO_x into Nitrogen and Oxygen. There are various ways this reaction can happen, but the most important factor is. NH₃. The reaction of NO_x with NH₃ to convert to Nitrogen and Oxygen has various chemical kinetics [7,10]. They are classified into three chemical kinetics category namely standard reaction (Eq.1), fast reaction (Eq. 2) and slow reaction (Eq.3) [2].



The standard reaction (Eq. 1) takes place in the SCR only if there is excess oxygen present. It is called standard because diesel engines usually run lean hence generally have excess oxygen present. The fast reaction (Eq. 2) takes place in the SCR when there is an equimolar concentration of NO and NO₂ present. The slow reaction (Eq. 3) occurs when only NO₂ is present in the SCR therefore it is of imperative importance to maintain as close to the

possible equimolar concentration of NO and NO₂ in the SCR for the effective functioning of SCR to reduce NO_x to N₂ and O₂ [2].

The advantages of the SCR and DPF are known separately but with ever-increasing stringent emission targets and cost-cutting in the industry, it was essential to come up with a single system that incorporates the advantages of both these after-treatment systems and as well as reduces packaging and component cost in a vehicle. This is where Selective Diesel Particulate Filter (SDPF) was introduced in after-treatment system to replace the functions of both SCR and DPF and perform it by a single system. In the SDPF the follow through walls of a traditional DPF is coated with SCR wash-coat material. PM and NO_x emissions need to be simultaneously improved. Insufficient light-off speed and space constraints make using SCR and DPF together in after-treatment system difficult. Integrated function of SCR coating on high porosity DPF reduces NO_x emission as well as controls the PM emission [19,20].

The standard measurement of soot on DPF or SDPF uses pressure differential sensors to measure the back pressure generated due to soot. Under empirical standard, models have been made and calibrated for the backpressure to predict the soot inside the catalyst, but these are not accurate [1]. Now due to tighter laws on emissions, it is of paramount importance to predict correctly the exact amount of soot inside the catalyst. This is where the radio frequency (RF) sensing technology comes into the picture. In this technology, electromagnetic waves are generated inside the catalyst and scanned over a frequency domain. These waves constructively interfere with each other forming various resonant peaks. This RF spectrum is sensitive to the changes in the dielectric properties of the catalyst and the amplitude and the resonant frequency of the resonant peaks can change as these properties change. Previous studies have shown that conductivity and dielectric property of a catalyst changes with change in amount of soot inside the catalyst [6,12,13]. Corporations like CTS and Amphenol have devised a fully integrated DPF sensor and control unit using RF sensing technology. They can measure soot and ash level directly in DPF as well as control after-treatment system operations. These sensors have been developed to be used on wide variety of vehicle types from passenger vehicles to commercial truck. This sensor can also be used on gasoline vehicles with a gasoline particulate filter. They can perform real-time measurement and onboard diagnostics as well as feedback control operation based on soot and ash level. Additionally, the RF technique has been used to measure NH₃ loading on the SCR catalyst [2,15,16,17,18]. In these reports, the changes in the dielectric properties of the catalyst due to changes in the ammonium ions on the SCR surfaces are monitored by changes in the RF resonant frequencies and the RF attenuation.

In this study, it was explored how the RF spectrum changes with the changes in both soot loading and ammonia storage inside the SDPF. As it is reported how soot load affects the RF response of the DPF and how NH₃ loading affects the RF response of the SCR, here we examine the influence of both on the SDPF [2,6,9,12,13]. We explore how the RF response to soot stored on the SDPF is affected by the simultaneous presence of stored NH₃. Temperature is also an important parameter to dielectric properties of the SDPF. Thus, an

investigation of the influence of temperature on the RF spectrum in the presence of soot and ammonia was performed. Finally, quantitative models to accurately predict the amount of soot and ammonia inside the SDPF separately as well as simultaneously were estimated. Limits to the predictions are discussed.

2 Literature review

There are two research papers that most closely resemble the work done in this experiment. They follow a similar procedure and observe similar parameters with respect to RF sensing in SDPF.

2.1 Detection of the ammonia loading of a Cu Chabazite SCR catalyst by a radio frequency-based method

This paper is written by Dieter Rauch, David Kubinski, Ulrich Simon and Ralf Moos. In this paper, they found the relation between ammonia loading on a chabazite SCR catalyst. Their procedure was to stepwise increase the temperature from 200° C to 350° C they registered the RF spectrum change with respect to temperature. They also concluded that with an increase in temperature due to change in conductivity and dielectric property the amplitude of the resonant peaks decreases. They then registered the RF spectrum at 250° C before injecting 500 ppm of ammonia and after the SCR was saturated with ammonia and they concluded that presence of ammonia changed the RF spectrum it reduced the amplitude of resonant peaks, the resonant peaks were formed at a lower frequency and they were less defined. Finally, they did a quantitative analysis of change in the quality factor that is the reduction in the intensity received at the receiver antenna with respect to transmitting antenna, in accordance with change in the ammonia storage per volume of catalyst at various temperatures. This shows the amount of ammonia stored at various temperatures as well as the RF spectrum change with change in ammonia loading. They demonstrated that RF based method can be used on a zeolite based SCR catalyst to measure the amount of ammonia storage on the SCR catalyst. They also reported that this technique could be used to improve the present control systems in the SCR and make it better and more active. The RF sensing is robust against varying feed ratio. They think this method could also be used to figure out active and acidic sites inside the SCR catalyst and give a reason as why these sites react differently.

2.2 Advanced RF Particulate Filter Sensing and Controls for Efficient After-treatment Management and Reduced Fuel Consumption

This paper is written by Harsha Nanjundaswamy, Vinay Nagaraju, Yue Wu, and Erik Koehler Alexander Sappok, Paul Ragaller, and Leslie Bromberg. In this paper, the analysis involved checking the RF sensor by Filter Sensing Technologies as a standalone soot load measurement sensor for after treatment sensors. The results obtained by this standalone sensor for soot loading were compared to the gravimetric results and from various other soot sensors like microsoot sensor. It was also tested to be the sensor on which regeneration controls were calibrated to work. they proved that their system led to better fuel-saving and better soot detection and can be the answer

for future Onboard Diagnostic solution for soot loading and could be the substitute of particulate matter sensors for the whole automotive industry. They showed a 30% improvement in efficiency can be obtained by using this RF sensor for regeneration by decreasing the total regeneration process time and by decreasing the number of regenerations that are performed during the life of the engine/after-treatment system. They also predict that because of this the DPF will last longer. Their sensor can also be calibrated for different materials that would be used in DPF other than what they used since RF sensor works with all types of materials. Again, they focused on one single resonant peak for the whole experimental testing and calibration of regeneration controls. They have also highlighted that pressure and model based particulate filter control have not been efficient under real-world driving conditions and that it is of paramount importance that better real-time particulate matter sensing which they have achieved using RF sensing technology. They have used the RF sensor out to control when to start the regeneration process and when to end it. They have also controlled the number of times the regeneration process should be carried out using the same principles. They show results which state that using this real-time based RF sensing for particulate matter they have reduced the time taken for regeneration process by 30 % which leads to a proportional decrease in the number of regeneration events that had to be carried out throughout the testing procedure. They conducted the experiment both in a test cell and on a vehicle.

3 Experimental Setup

3.1 SDPF

The SDPF used in soot measurement was 4.4 cm diameter by 17.4 cm in length, cored from a larger piece used in a serial application. It was mounted tightly near the center of a stainless cavity, 31 cm long. An antenna was positioned between each face of the SDPF, till the center of the core and stainless screens defining the cavity's ends on each side.

3.2 Test Phases

The whole of the experiment comprised of multiple tests. Each test is a replicate of the other. The Test was divided into two phases namely the preparation phase and the testing phase.

3.2.1 Preparation Phase

The objective was to figure out how the Radio Frequency Spectrum changed with soot loading. To achieve this objective, the amount of soot that had to be present inside the SDPF had to be known. The Preparation phase comprised of loading known amount of soot in the SDPF. The empty SDPF was loaded with soot at room temperature using a benchtop Jing miniCAST 5201C soot generator. The mean mobility diameter of the generated soot was approximately 100 nm. The output of the soot generator was diluted with N₂. A Pump was used to generate a flow of 90 l/min for loading the soot. This flow was passed through the SDPF for soot accumulation. A filter was attached after the SDPF which removed any excess or large particles. A flow meter was added in the link to keep a check on the flow. Finally, the gases were passed through the snorkel into the exhaust. AVL microsoot sensor probes were attached upstream and downstream of the SDPF. The measured soot concentration was near 10 mg/m³. Additionally, two pressure sensors were added upstream and downstream of the SDPF to calculate the pressure drop due to soot loading as a precaution for a closed control feedback loop.

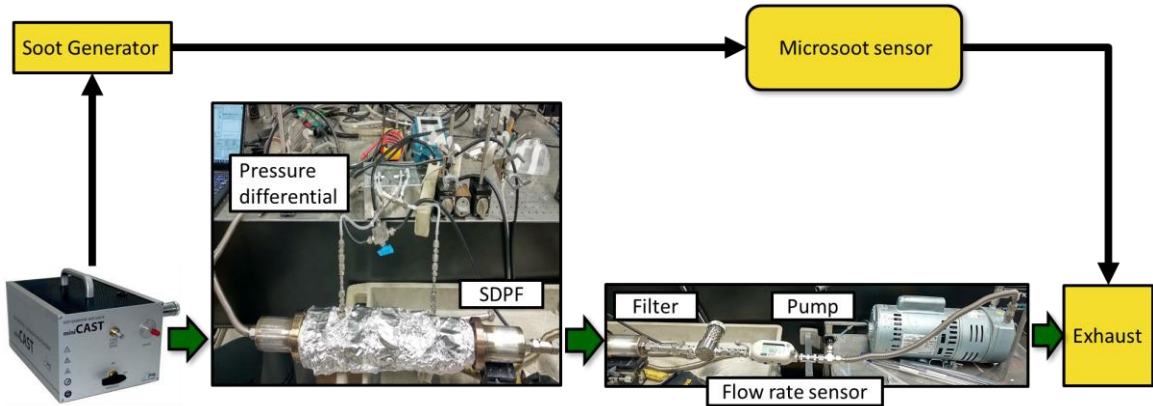


Figure 1: Preparation Phase Setup with SDPF

3.2.2 Testing phase

The SDPF is the part of the after-treatment system in exhaust. It was of utmost importance to simulate the exhaust environment inside the SDPF for getting realistic results. To achieve this heated gas-flow bench was set up with 5 MKS mass flow controllers controlling the amount of O_2 , NO_2 , NH_3 and N_2 through the SDPF. A Bronkhorst water injection system was used to supply 0.963 g/min of water vapor to the SDPF, which was 2% (by volume) of the total gas flow. The cavity containing the sooted SDPF, was then connected to this 60 L/min heated gas-flow stream. Thermal transducers were placed upstream and downstream of the SDPF. For determining the temperature dependence of the sooted DPF as well as the influence of stored ammonia, testing was done in a 5% O_2 and 2% water-gas mixture. Commercially available NTK NO_x sensors were also attached upstream and downstream of the SDPF. National Instruments hardware and software was used to collect the data from the mass flow controllers, NO_x sensors and transducers. Two stainless steel antennas were placed inside the cavity, one before and after the SDPF and each located roughly equidistant between the end-face of the SDPF and the reflecting screen. The RF S21 transmission parameter, the power received at the 2nd antenna with respect to the 1st, was measured in lean gas using an Agilent E5071C network analyzer. The gas coming out of the SDPF was sampled by a MIDAC FTIR to give feedback about the concentration of various gasses flowing through the SDPF. Finally, all the gas was directed to the exhaust for removal from the setup area.

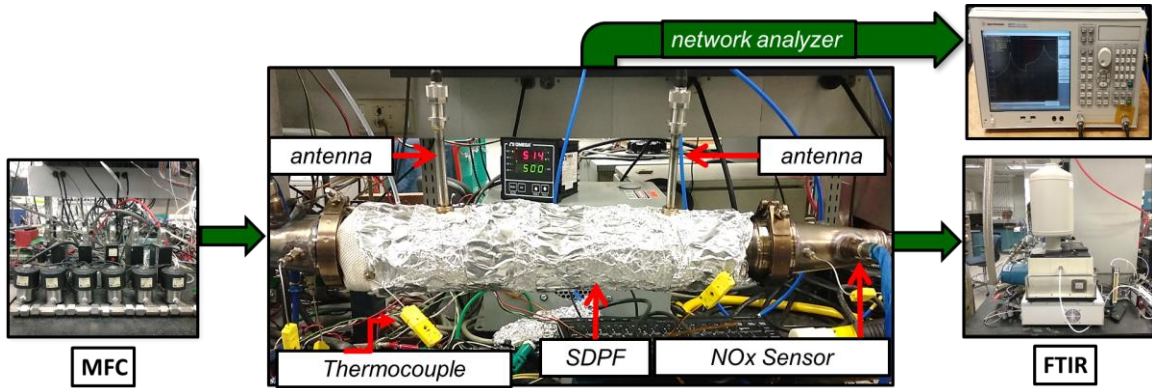


Figure 2: Heated Gas bench test setup

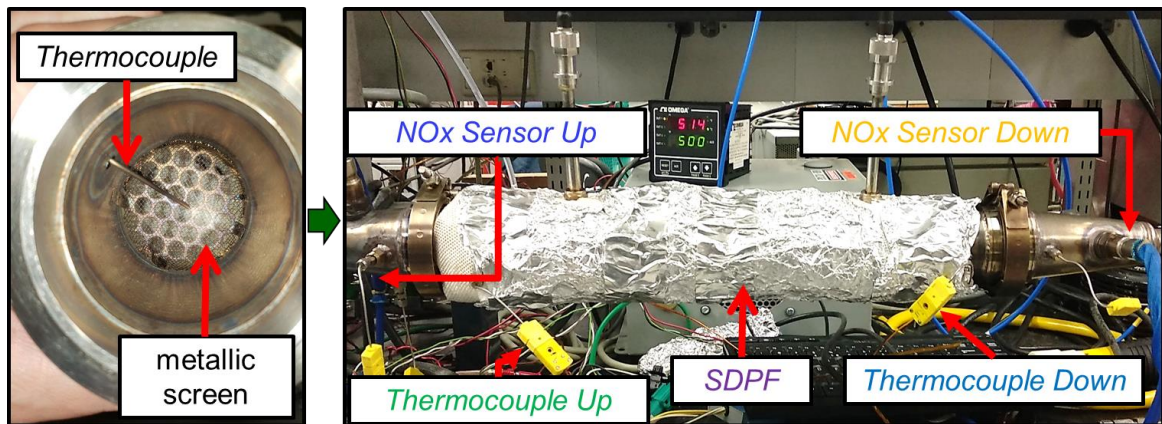


Figure 3: Interior and Exterior of the SDPF

3.3 Experiment Procedure

To give a broader idea about the procedure for conducting each test. The following procedure coupled with the temperature profile below highlight each step taken in the testing procedure.

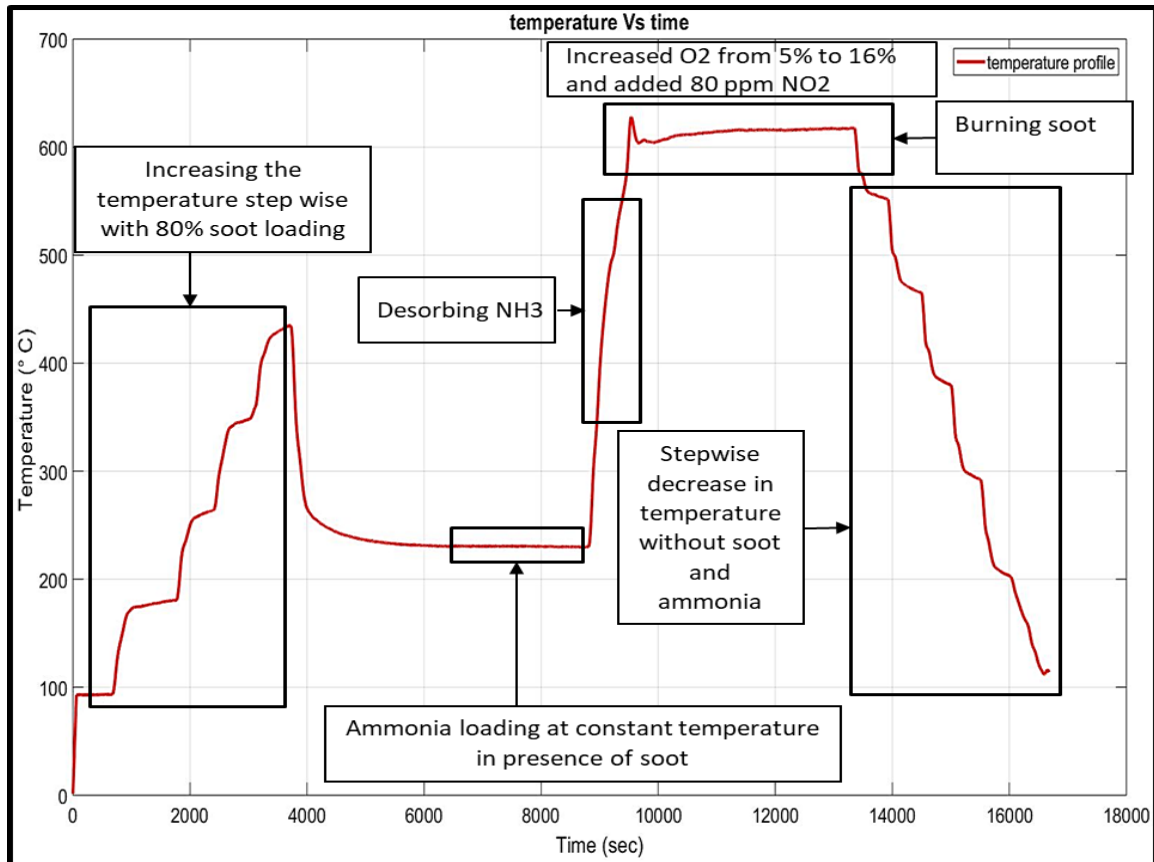


Figure 4: Procedure for the test with respect to temperature profile

- Load the SDPF with the required amount of soot and set up the apparatus.
- Increase the temperature in steps till 500°C to observe the change in the spectrum due to temperature change.
- Decrease the temperature to 250°C let it stabilize.
- Once stabilized, start injecting ammonia in at 400 ppm, wait till the SDPF is completely saturated with ammonia. This helps to capture spectrum change with respect to change in ammonia loading
- After SDPF is saturated with ammonia Increase the temperature till 650°C to desorb ammonia and increase oxygen concentration and add 80 ppm of NO_2 to aid to burn the soot away.
- Once the spectrum peaks are completely visible and stabilized, then decrease the temperature stepwise till room temperature to collect the RF spectrum for validation purposes

3.4 Radio Frequency Spectrum

To give a brief idea about RF sensing on a SDPF. Figure 5 represents a metallic enclosed area containing the SDPF which has receiver and transmitter antenna at either side. The transmitting antenna generates electromagnetic waves that reflect through the metallic

screen and lead to constructive interference which generates various resonant frequencies. This data is collected by the receiver and sent to the network analyzer which converts it to a spectrum. when Soot and ammonia loading changes, this leads to a change in conductivity and dielectric property of SDPF which eventually leads to a change in the peak resonant frequency. The intent was to capture this change in the RF spectrum and measure soot and ammonia loading.

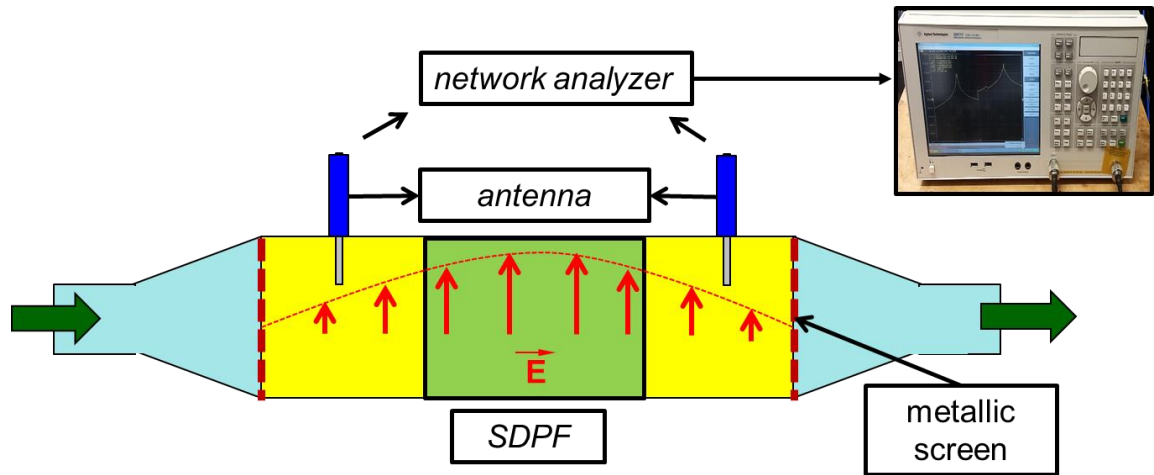


Figure 5: SDPF with RF antenna and TE₁₁₁ Resonant EM wave

Figure 6 shows a single RF spectrum with various resonant peaks scanned over a frequency of 2.5 to 5.5 GHz. TE₁₁₁ is the first resonant frequency, TE₁₁₂ is the second resonant frequency and TE₁₁₃ is the third resonant frequency a proper detailed layout of how these resonant peaks are formed under constructive interference is shown in figure 7.

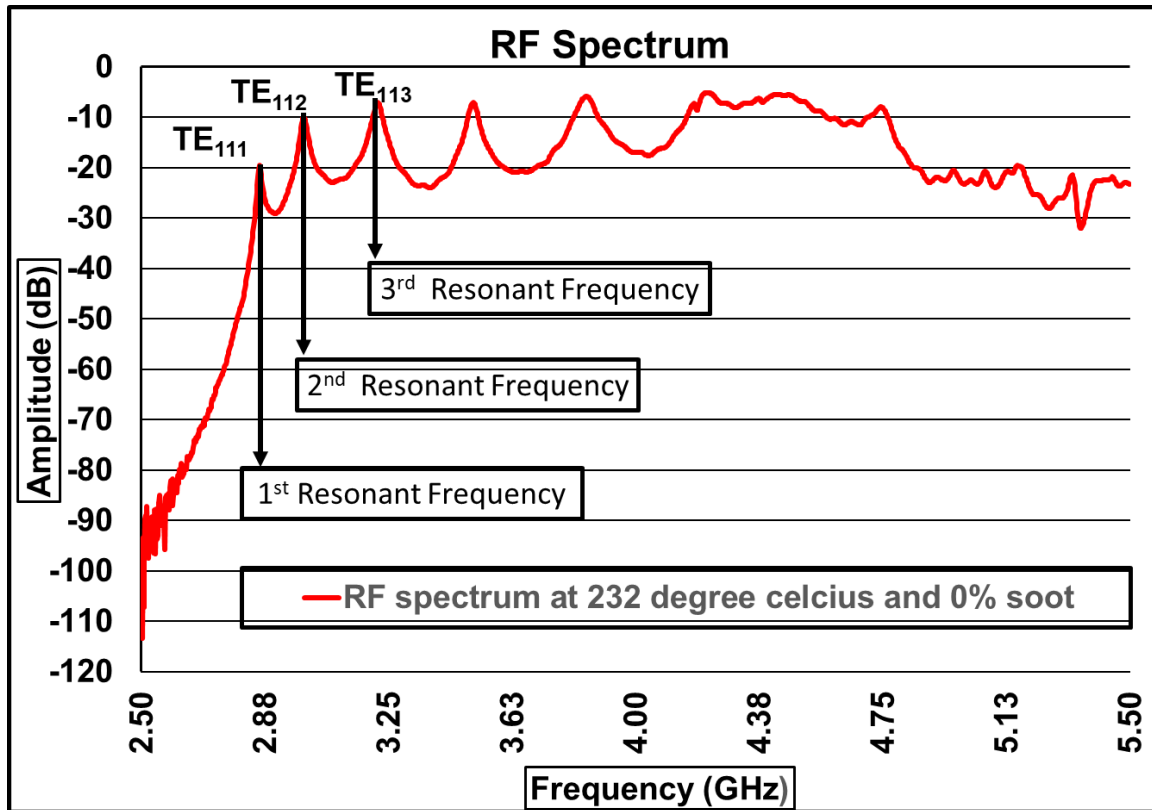


Figure 6: RF spectrum with various resonant peaks

The RF spectrum without any soot is shown in Figure 6. It represents the energy transmitted by the upstream antenna to the downstream antenna as the frequency is scanned. If all energy is transferred, then the amplitude value will be higher close to 0 dB, anything lower than that means lesser energy is being transferred (attenuation). It is visible that the peaks developed over the frequency range are the amplitude of the resonant modes. The first peak refers to the Transverse electric 111 mode which as shown in figure 7 is the resonant mode when 1 half wavelength is generated. similarly, for the 2nd and the 3rd modes from figure 7, they are the resonant modes when 2 and 3 half wavelengths are generated. the peaks get less developed as scanning frequency is increased this is due to multiple resonant modes interfering with each other and hence making those peaks impossible to analyze.

The RF spectrum that we see in Figure 6 is the processed signal generated by the network analyzer. The actual input is very different. The circle fit method^[22] and 3 dB^[22] method as explained by Paul J. Petersan and Steven M. Anlage in their research "Measurement of resonant frequency and quality factor of microwave resonators: Comparison of methods"^[22] is used to get the final RF spectrum as we see in all the figures in this research.

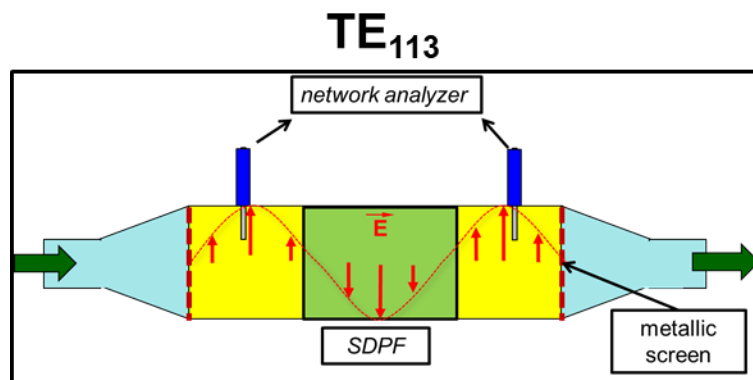
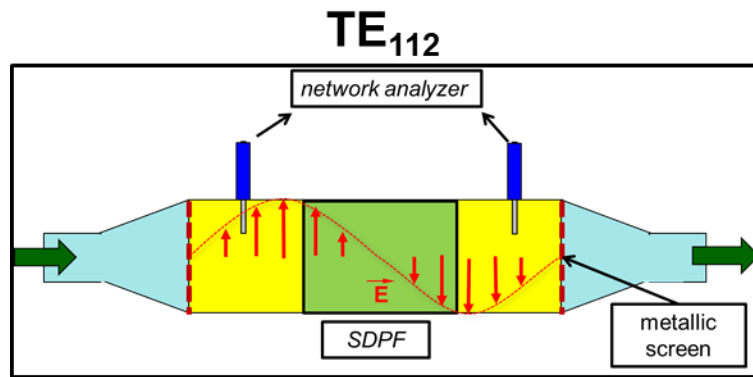
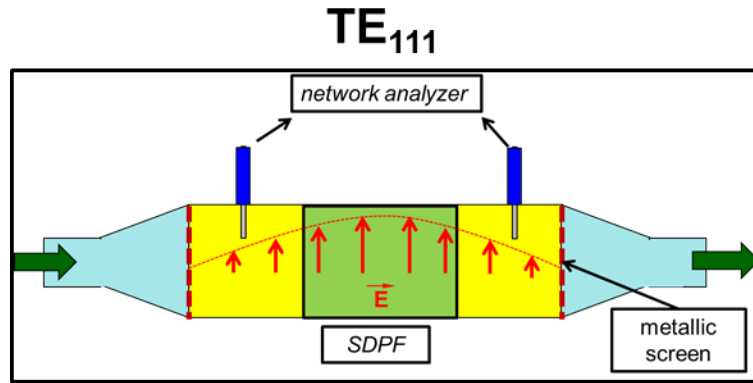


Figure 7: Resonant modes inside SDPF

3.5 Test Cases

For the experiment 8 cases were ran of soot loading. The soot loading was increased from 0 % of max soot loading to 76 % of max soot loading, where 76% soot loading refers to 1.37 grams corresponding to 5.2 g/l soot on the SDPF. It took 24 hours of monitored soot loading for the maximum soot loading case under the constant parameters. It is amazing to see how a small quantity of 1.37 grams which corresponds to 76% of the maximum soot loading case could take such a long time to load up. To give a clearer view of the test cases, they are classified into 2 parts, that is light loading and heavy loading. Soot loading of less than 10 percent is referred to as light loading and above 10 % as heavy loading.

| Case Number | grams of soot loaded | % of max soot loading | time taken to load soot |
|-------------|----------------------|-----------------------|-------------------------|
| Case 0 | 0.00 g | 0% | 0 hours |
| Case 1 | 0.05 g | 2.8% | 50 minutes |
| Case 2 | 0.14 g | 7.6% | 2 hour 30 minutes |
| Case 3 | 0.18 g | 10.0% | 3 hours |
| Case 4 | 0.41 g | 22.7% | 6 hours 50 minutes |
| Case 5 | 0.73 g | 40.0% | 12 hours |
| Case 6 | 0.76 g | 42.0% | 12 hours 20 mins |
| Case 7 | 1.37 g | 76.0% | 24 hours |

Table 1: Experimental cases

During the preparation phase, the MiniCast was kept at Cast 1 setting for loading up SDPF soot for all the cases which give us constant output in soot particle size of ≈ 100 nm and flow was kept constant at 90 L/min which gave an average concentration of soot inside the flow as 11g/hr.

| Constants | | | |
|-----------|-----------------------|------------------|--------------|
| Flow Rate | Average concentration | Soot size | Cast setting |
| 90 L/min | 11 g/hr | ≈ 100 nm | Cast 1 |

Table 2: Constant parameters in preparation and testing phase

4 Results and Observations

4.1 RF spectrum interaction with soot

The priori hypothesis was that the presence of soot changes the dielectric property inside the SDPF and hence should produce change to the RF spectrum. Also, from previous studies conducted using RF spectrum on the three-way catalyst and in presence of ammonia [2], it is known that RF spectrum changes due to the change of dielectric property due to the presence of ammonia [2]. To evaluate these changes, eight test cases were generated with gradually increasing soot concentration inside the SDPF as listed above in table 1.

In figure 8 soot 0 refers to 0% soot loading of maximum soot loading, soot 2.8 refers to 2.8% soot loading case and so on. From figure 8 it is visible that increasing the amount of soot loading in SDPF, the RF spectrums move down and to the left. In other words, the amplitude of the resonant peak decreases and resonance is attained at a lower frequency. It is also observable that as soot is increased inside the SDPF the resonant peaks start disappearing and after 22.6% soot loading case these resonant peaks completely disappear that is no analysis can be performed on the resonant peaks. There is no more information about these peaks but, the baseline spectrum is still moving down with increasing soot loading and this can be used to say something about the soot loading condition.

In the light loading cases, the resonant peaks are clearly visible and separated for each soot loading. Hence, these peaks can be used to quantify soot loading. transitioning to heavy loading, the threshold is reached, 22.6 % case where the peaks are lost, in such cases, it is of imperative importance to analyze the spectrum using its baseline spectra to quantify soot loading.

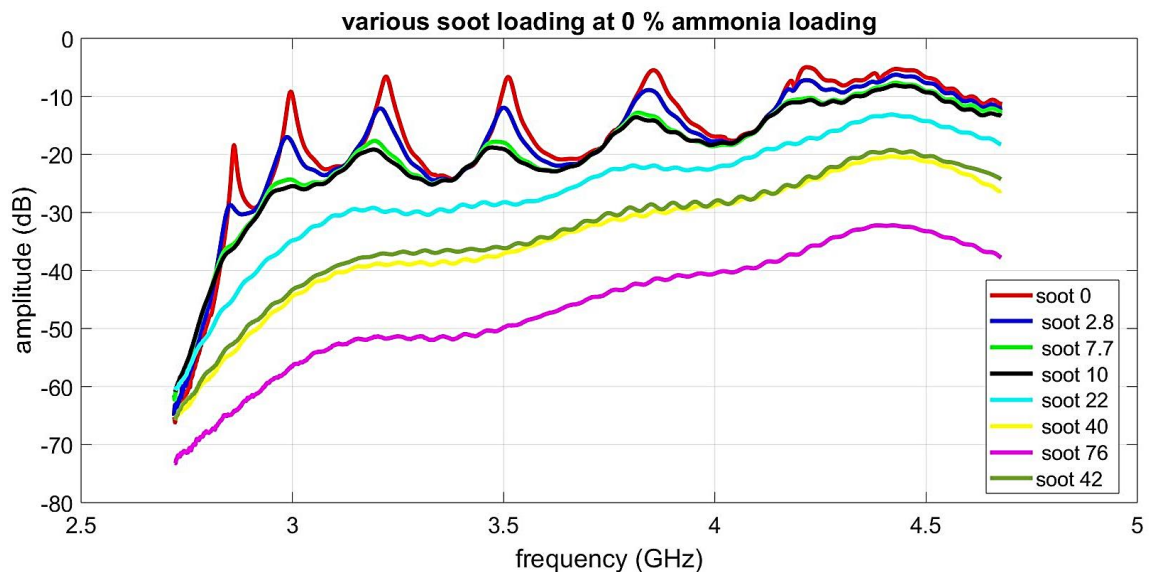


Figure 8: RF spectrum comparison for various soot loading cases at 228° C

4.2 Temperature dependence of RF spectrum in presence of Soot

From previous studies it is known that that the temperature is a really important factor with respect to the dielectric property [4, 5]. When temperature changes, it changes the dielectric property inside the SDPF hence influencing the RF spectrum. When temperature is referred, it means the mean temperature of the upstream and downstream temperature transducers.

$$\text{Mean temperature} = \frac{\text{thermocouple upstream} + \text{thermocouple downstream}}{2} \dots\dots\dots(4)$$

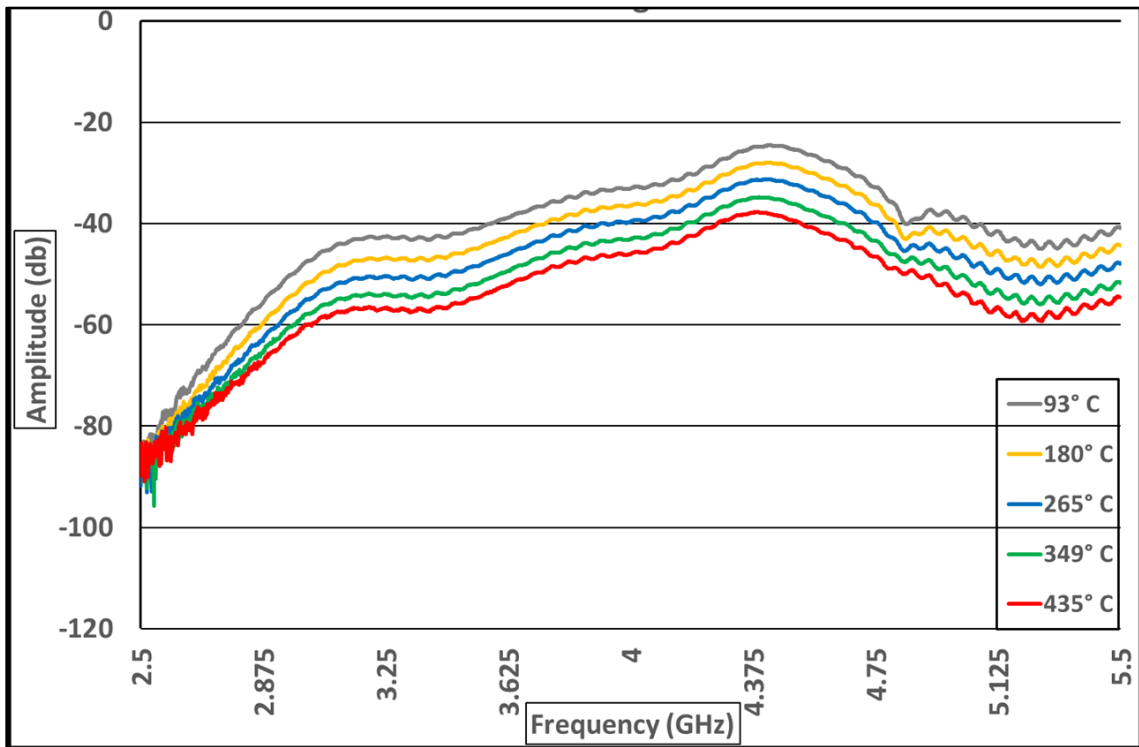


Figure 9: temperature dependence of RF spectrum for 76% soot loading case

As discussed, temperature is one of the most important parameters that affect the RF spectrum. Figure 9 represents the variation in RF spectrum at different temperatures for 76% soot loading case. The figure highlights the change in RF spectrum at 76 % soot loading with stepwise increasing change in measured temperatures. The measured temperature is the same mean temperature that is referred above, this is done because there is as much as 100°C measured temperature gradient between the thermocouples at higher temperatures

At 76 % soot loading, the resonance spectrum decreases in intensity as the mean SDPF temperature is raised. This is again due to the increased dielectric properties inside the SDPF.

Figure 10 has four figures associated here showing the temperature variation for RF spectrum for four soot loading cases. Figure 10. A shows the temperature variance of RF spectrum when there was no soot present. Figure 10. B shows the temperature variance of RF spectrum for light loading 10% soot loading case. Figure 10. C for 40% soot loading and Figure 10. D for 76% soot loading case when the temperature is varied. The main point in this comparison is that in presence of soot loading, as the temperature was increased, baseline spectrum moves down i.e. decreases in intensity, but this decrease is dependent on the amount of soot loading. As the soot loading is increased the change in the amplitude of the baseline spectrum due to temperature variation also increases. This change is visible in the figure 10 below as moving from 0% soot loading to 76 % soot loading the temperature variations start becoming more prominent.

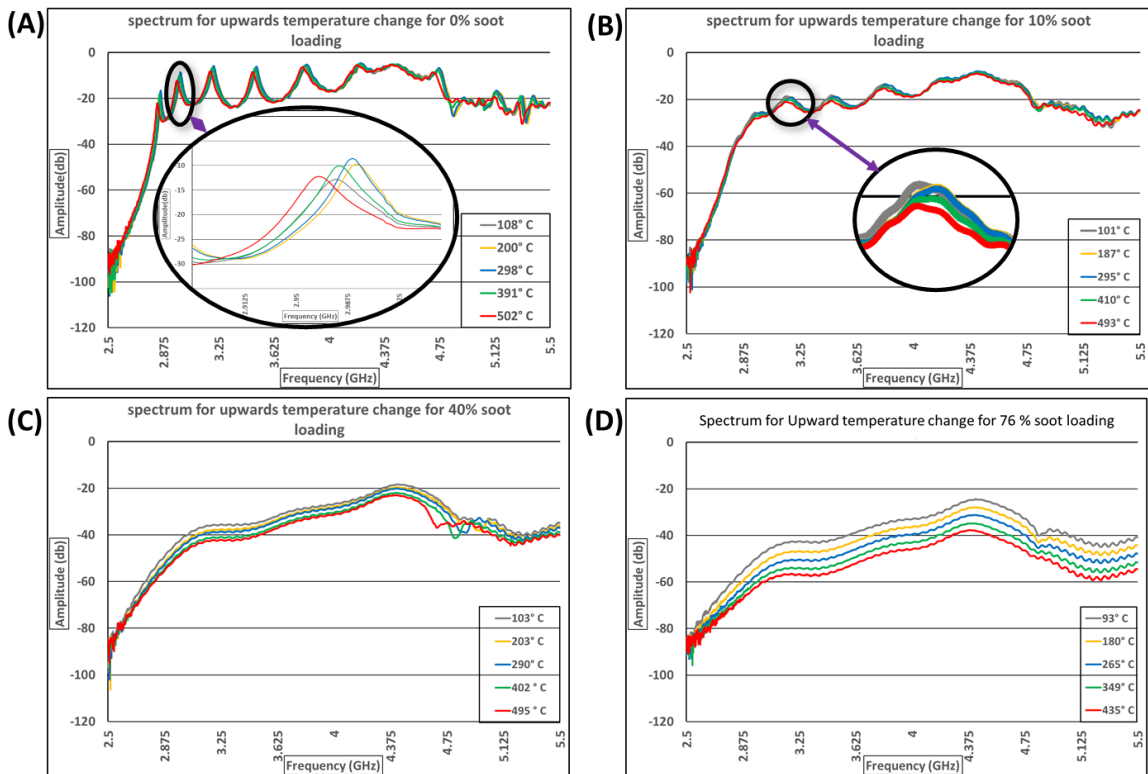


Figure 10: RF spectrum variation with respect to temperature for various soot loading cases. (A) RF spectrum change with respect to temperature for 0% soot loading case. (B) RF spectrum change with respect to temperature for 10% soot loading case. (C) RF spectrum change with respect to temperature for 40% soot loading case. (D) RF spectrum change with respect to temperature for 76% soot loading case.

4.3 RF spectrum interaction with ammonia

In each test the temperature was increased stepwise from 100° C to 500° C in steps of 100°C to evaluate the RF spectrum change with respect to temperature. Later the temperature was reduced to 250° C and stabilized before injecting 400 ppm of ammonia which approximately corresponded to 0.4 g of ammonia storage in the SDPF. The following figures explain how the RF spectrum changes with ammonia loading.

In Figure 11 the overlay graphic shows the output of upstream and downstream NO_x sensors. The red line is the output of the upstream NO_x sensor and the blue line is the output of the downstream NO_x sensor it is visible how the upstream NO_x sensor registers the ammonia input immediately as it is placed before the SDPF and downstream NO_x sensor registers the difference in ammonia storage. When the SDPF is saturated ammonia input was shut off. the upstream and downstream register this change in a similar manner as described above. The RF spectrum in yellow signifies the condition before ammonia input was initiated and the RF spectrum in green signifies the condition after the SDPF was saturated with 400 ppm of ammonia (approximately 0.4 g of ammonia storage). It is visible that the two spectrums are different. The spectrum after saturation of SDPF with ammonia has shifted down, to the left and the resonant peaks are less defined as compared to the RF spectrum before ammonia loading. This means that there is a decrease in amplitude of resonant peaks, the peaks are formed at lower frequency and that there is an increase in the dielectric properties inside the SDPF.

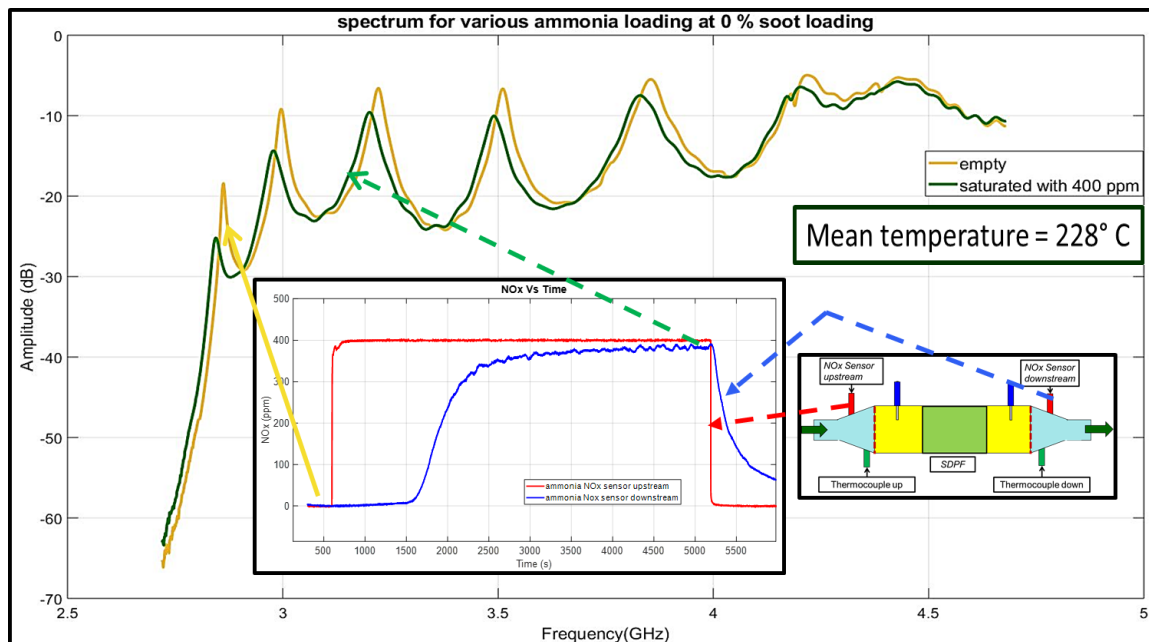


Figure 11: RF spectrum change under various ammonia loading condition at 0% soot loading

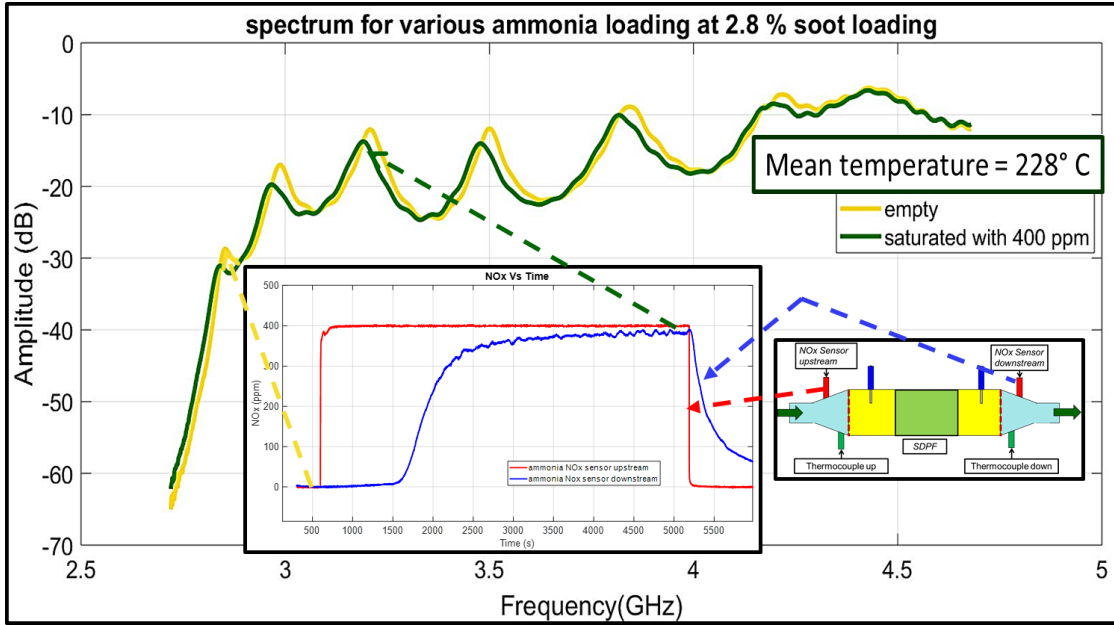


Figure 12: RF spectrum change under various ammonia loading condition at 2.8% soot loading

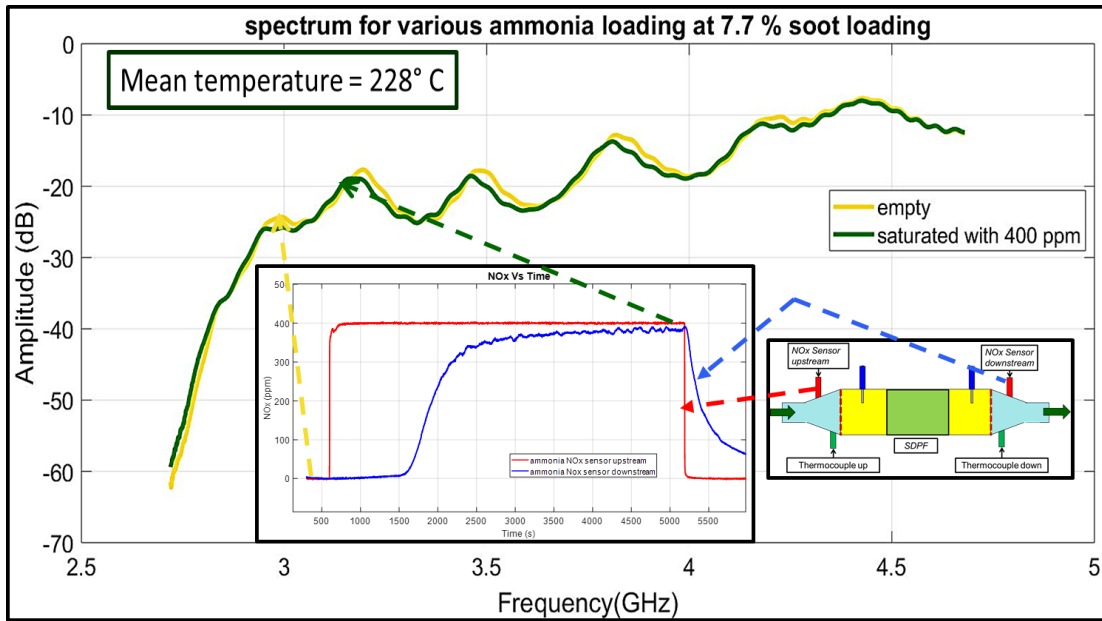


Figure 13: RF spectrum change under various ammonia loading condition at 7.8% soot loading

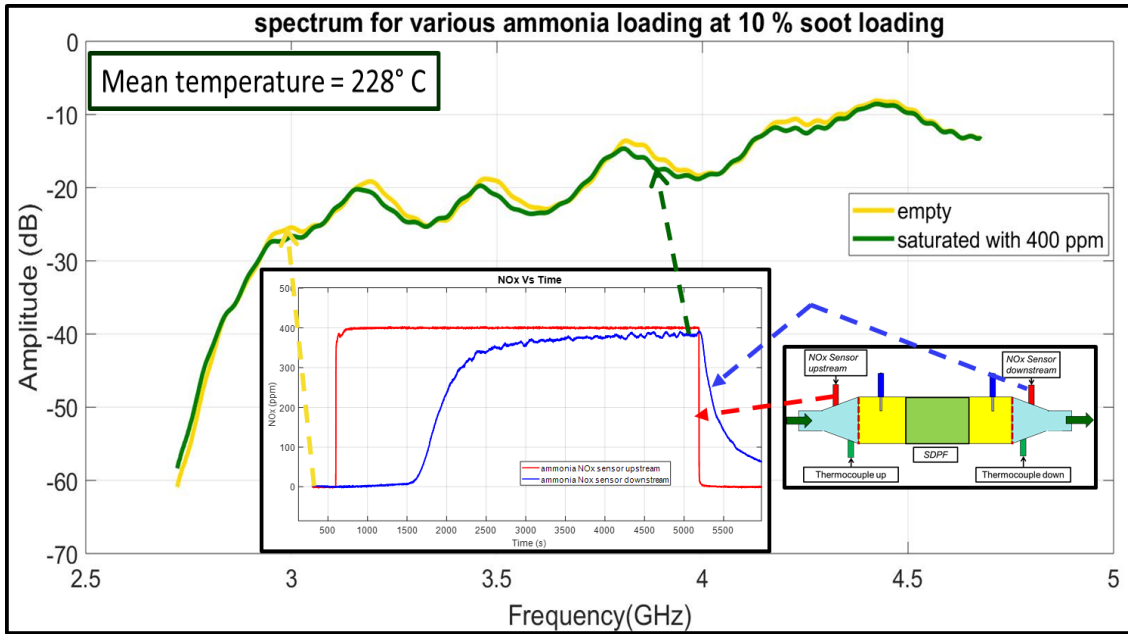


Figure 14: RF spectrum change under various ammonia loading condition at 10% soot loading

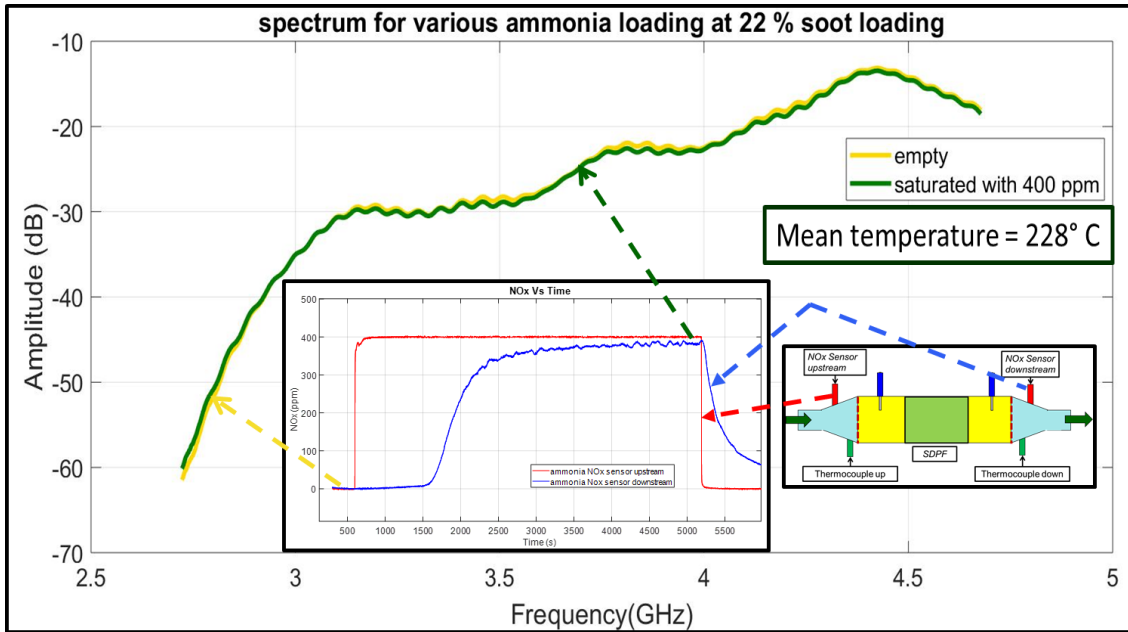


Figure 15: RF spectrum change under various ammonia loading condition at 22.6% soot loading

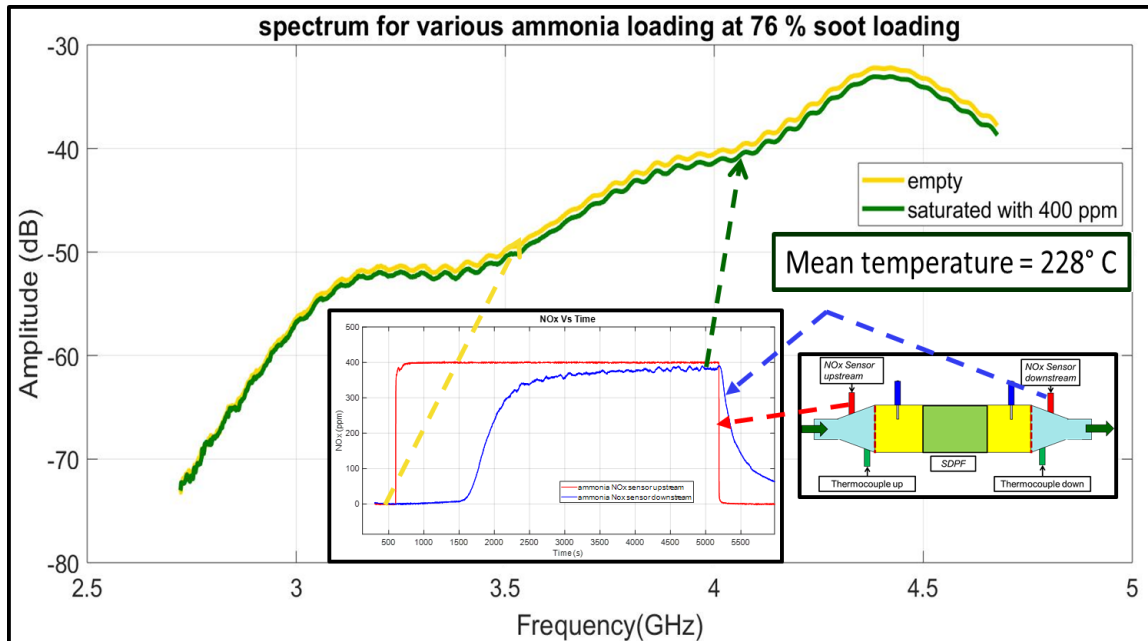


Figure 16: RF spectrum change under various ammonia loading condition at 76% soot loading

As the soot loading is increased, from Figure 12, for the 2.8% soot loading case, it is observed that the spectrum has shifted down and to the left for saturated ammonia loading condition compared to when the SDPF was empty of ammonia but, this shift compared to 0 % loading is lower. Similarly increasing the soot loading in Figure 13 the trend is still present, but the shift compared to less soot loading case is lower. In Figure 14 at 10% soot loading there is shift in the spectrum due to change in ammonia loading but, the important point to notice here is that the first resonant peak is lost. This concludes that ammonia influences the light loading cases. Going to the heavy loading cases as shown in Figure 15 at 22 % soot loading the spectrum with and without ammonia is nearly the same and there is no change in the RF spectrum due to ammonia that can be registered here. Similarly, in Figure 16 for the 76 % soot loading case there is a negligible effect of ammonia loading on the RF spectrum.

From these observations, it can be confidently said that to conduct a quantitative analysis of both ammonia and soot simultaneously at an instant can only be performed under light soot loading cases that is for soot loading of less than 10% of maximum soot loading because the RF spectrum registers a significant change in presence and absence of ammonia for these cases. In subsequent sections, the quantitative measurement techniques that can be used to simultaneously calculate soot and ammonia loading at low loading case, to calculate the amount of soot present at various temperature and show that in summation ammonia's effect can be neglected on the RF spectrum change under soot loading condition have been explained.

4.4 Verification for running each test empty of any soot and ammonia from previous test

It was of imperative importance to start all tests with an empty SDPF which has no ammonia storage nor any soot loading leftover from the previous test. In Figure 17, the Figure 17. A shows the RF spectrum before burning away the soot and desorbing the ammonia for various soot loading condition and the Figure 17. B shows RF spectrum after burning away the soot and desorbing the ammonia for the same soot loading condition, both at 200° C measured temperature. It is visible that the spectrums were separate and different before burning away the soot and once the soot was burned away the RF spectrum for the various soot loading cases overlap. This shows us that the SDPF is empty of soot and ammonia and has returned to the same state.

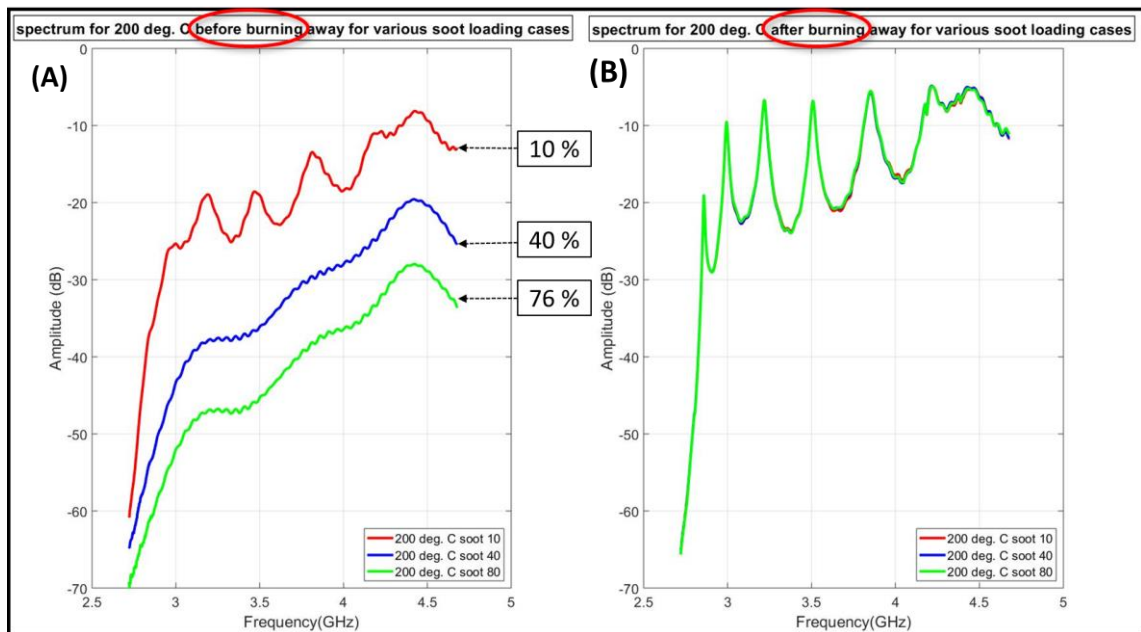


Figure 17: Validation for running each test empty of soot and ammonia in SDPF. (A) RF spectrum for various soot loading cases at 200° C when the SDPF was saturate with ammonia. (C) RF spectrum for various soot loading cases at 200° C after soot was burned and ammonia desorbed.

It was also required to verify that after we increased the temperature stepwise from 100° C to 500° C in steps of 100° C, we did not burn away any soot from the SDPF. Figure 18 shows three RF spectrums for the 76% soot loading case. The RF spectrum in red is the spectrum at 180° C when we were increasing the temperature. The RF spectrum in blue is the spectrum at 264° C when we were increasing the temperature. The RF spectrum in black is the spectrum at 230° C after temperature dependency analysis was conducted and the temperature was decreased to 250° C and before ammonia was injected inside the

SDPF. We see that the spectrum at 230° C lies between the other two spectra hence we can say that no soot has been burned from the SDPF while we were increasing the temperature.

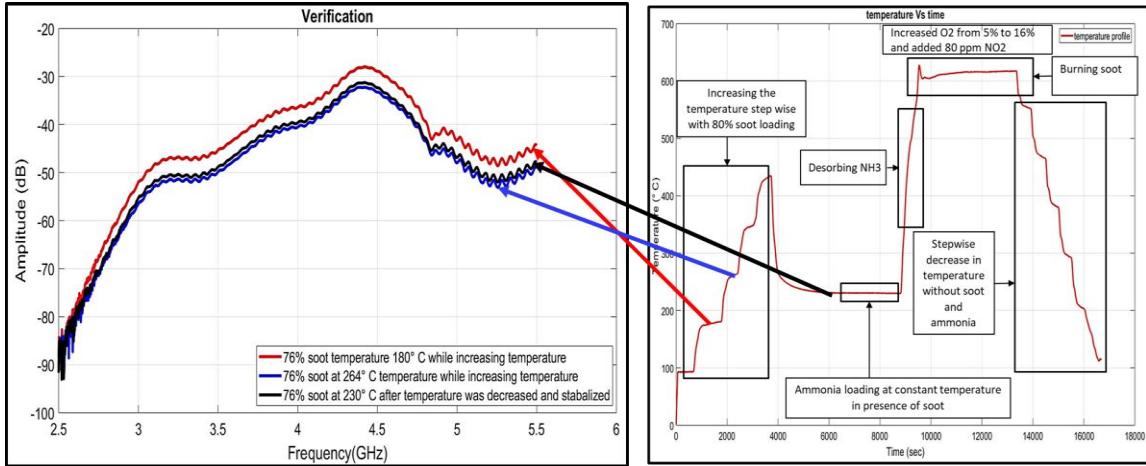


Figure 18: Verification that no soot was burned after RF spectrum temperature dependence analysis

4.5 Quantitative Analysis of soot loading and ammonia storage

As mentioned at the end of section 4.3 quantitative analysis was conducted for simultaneously calculating soot and ammonia loading for the four light soot loading cases, to calculate the amount of soot present at various temperature and to show that when both soot and ammonia is present inside the SDPF, the ammonia's effect on the RF spectrum can be neglected for the heavy soot loading cases.

It is considered that during the calculation of the amount of soot loaded on the SDPF there is uncertainty of $\pm 10\%$ of the calculated value. This uncertainty is created due to factors involved with test setup, apparatus and test procedure variability.

4.5.1 Quantitative measurement of soot loading at various temperatures

To quantitatively estimate the amount of soot present in the SDPF at a particular temperature using RF spectrum, the most important factor was the RF spectrum at that particular temperature and soot loading. Figure 18 shows the RF spectrum for 76% soot loading case at various temperatures that were registered as the temperature was increased stepwise. A large frequency domain was selected such that it can account for most of the resonant peaks, in cases where resonant peaks were available, and the frequency domain that was selected was 2.8 GHz to 4.6 GHz. This was done so that the baseline spectrum could be analyzed for all our cases. Each RF spectrum was made up of 1601 data points having unique amplitude and frequency. The mean amplitude of the spectrum in this range was calculated at each temperature step using the equation (5) as stated below. The same procedure for all the cases was carried out. Figure 19 shows the temperature dependence of the mean amplitude of the spectrum for all the soot loading cases at various temperature

over the selected frequency range and Figure 20 shows the linearly interpolated data that shows how the mean amplitude changes as a function of soot loading at a constant temperature. For example, if SDPF was operating at a constant temperature of 400° C and the mean amplitude over this frequency domain was approximately 28 decibels then the soot loading at that instant will nearly be 0.41 g or as that corresponds to nearly 22.7% of maximum soot loading. This way RF sensor can be calibrated to read the amount of soot loading under given temperature condition.

$$\text{Mean Amplitude of Spectrum} = \frac{\sum_{i=1}^n (\text{Amplitude at point } i)}{n} \dots\dots\dots(5)$$

$n = 1601$

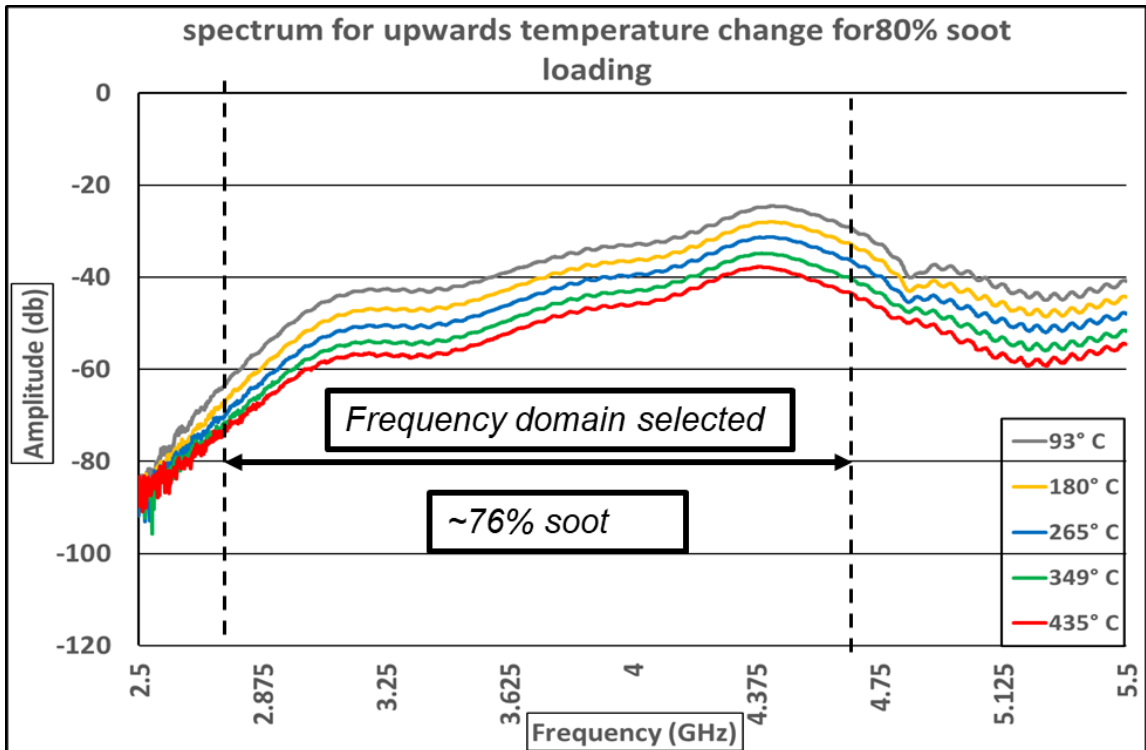


Figure 19: Frequency domain selection for 76% soot loading case for quantitative measurement of soot loading at various temperatures

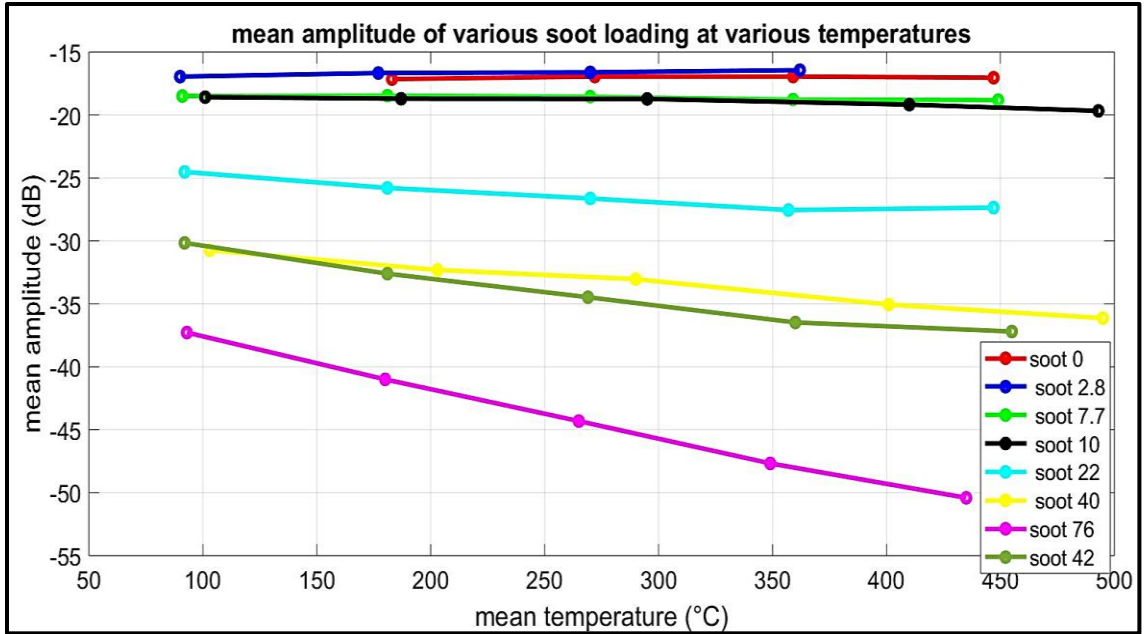


Figure 20: Mean amplitude of all soot loading cases at various temperature for the frequency domain selected

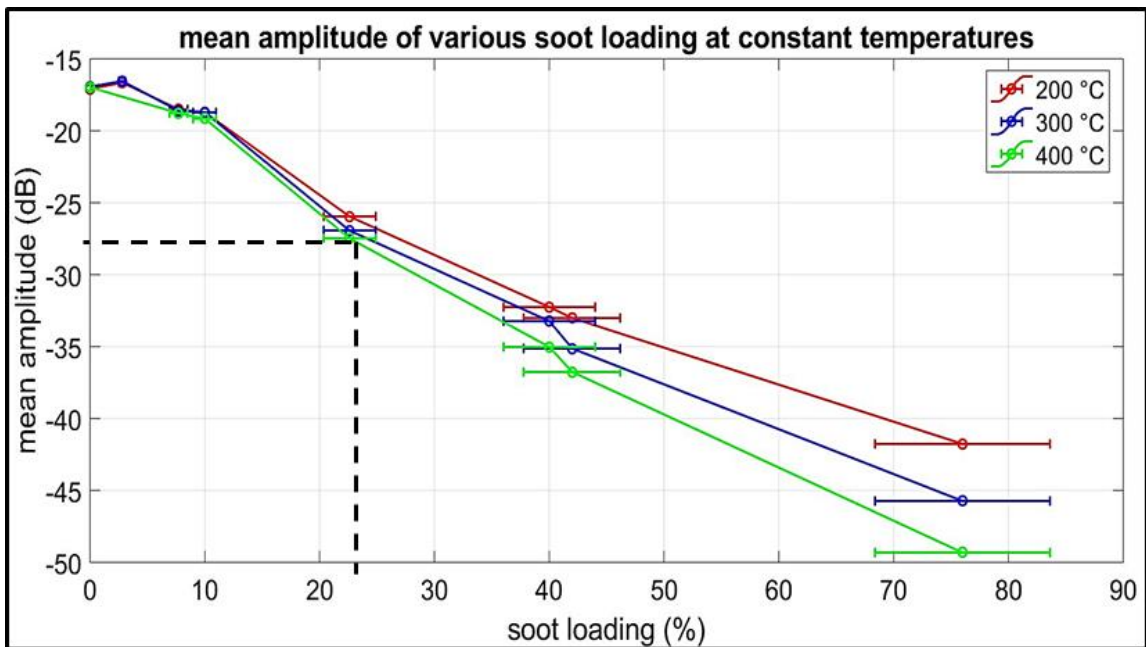


Figure 21: Quantitative model for estimating soot loading when mean amplitude and the instantaneous temperature is known

4.5.2 Quantitative analysis of ammonia's effect on the RF spectrum change under various soot loading condition.

To quantitatively estimate the effect of ammonia on RF spectrum in presence of soot the RF spectrum in each soot loading case before ammonia was injected i.e. the empty state and after the SDPF was saturated with ammonia was registered. In figure 19 there are two plots, the plot on the left shows RF spectrum at 228° C for all the soot loading cases when no ammonia was injected. A large frequency domain to analyze this spectrum was selected to consider all the resonant peaks so that the effect on both light soot loading and heavy soot loading cases can be observed. The frequency domain selected was 2.8 to 4.66 GHz. The mean amplitude of these RF spectra over this frequency domain was calculated using equation (5). This was done for both the cases, before ammonia loading and after SDPF was saturated with ammonia. The figure on the right in figure 19 shows two data sets. The blue line indicates the mean amplitude of the RF spectrum in the selected frequency domain for all soot loading cases when the SDPF was saturated with ammonia and red line indicates when SDPF is empty of ammonia i.e. before ammonia was injected in SDPF. It is visible that these two lines overlap at all the testing points. In conclusion, there cannot be shown any difference between the empty and saturated ammonia loading cases. Hence, ammonia loading has no effect on RF spectrum in the presence of soot within experimental certainty

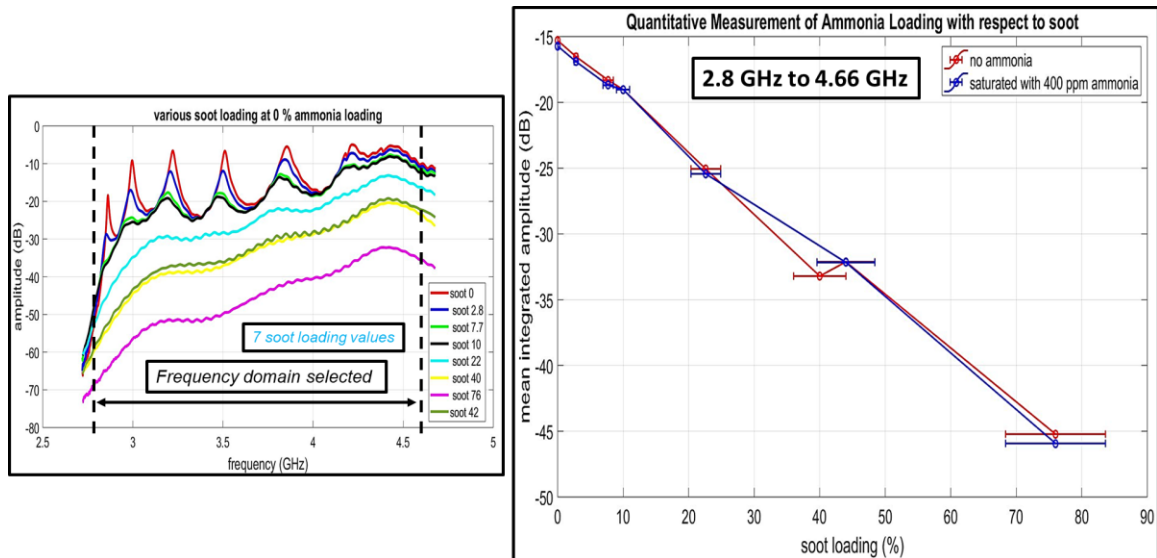


Figure 22: Quantitative analysis of ammonia's effect on the RF spectrum change under various soot loading condition and large frequency domain

To verify if the conclusion that, ammonia loading has no effect on RF spectrum in the presence of soot within experimental certainty was true, a smaller frequency domain was also selected and analyzed. If it showed the same trend, then we would conclude that ammonia does not show any effect on the RF spectrum in the presence of soot. This time the same analytical process was repeated but instead a smaller frequency domain i.e. 4.33 to 4.66 GHz was taken. Figure 22 shows the results for this analysis and like the large frequency domain it can be concluded that it does not show any difference between the

empty and saturated ammonia loading cases. Hence, ammonia loading has no effect on the RF spectrum in the presence of soot within experimental certainty

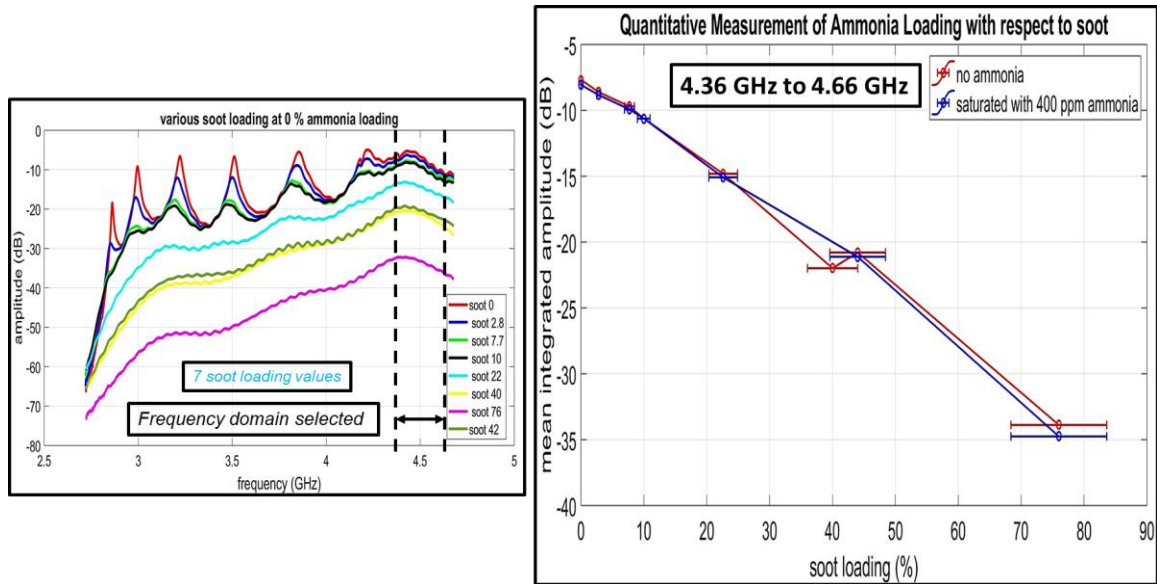


Figure 233: Quantitative analysis of ammonia's effect on the RF spectrum change under various soot loading condition and small frequency domain

4.5.3 Quantitative analysis for simultaneously calculating soot and ammonia loading at light soot loading cases.

Under light soot loading conditions, it can be observed that resonance peak is visible. The 4th resonant peak was the most defined for all the cases in the light soot loading group that is from 0% soot loading to 10% soot loading of maximum soot loading. In Figure 23 the Figure 21. B shows the RF spectrum of various soot loading cases in absence of ammonia that is before ammonia was injected and the 4th resonant peak was selected within frequency domain of 3.35 to 3.65 GHz. The same procedure was done for light soot loading cases when the SDPF was saturated with ammonia. Figure 23. B shows the RF spectrum in red which signifies the 4th resonant peak for various light soot loading cases and before ammonia was injected that is SDPF was empty of ammonia. The RF spectrum in blue signifies the 4th resonant peak for various light soot loading cases and after the SDPF was saturated with 400 ppm of ammonia. The mean amplitude of these two cases was recorded i.e. with and without ammonia under various soot loading cases. The frequency at which the resonant peaks are formed for these two groups was also recorded. Figure 23. C shows how the mean amplitude of the selected resonant peak varies with soot loading for the two groups, where SDPF was empty and saturated with ammonia. Figure 23. D shows how the resonant peak frequency varies with soot loading for the two groups where SDPF was empty and saturated of ammonia. If the mean amplitude of the 4th resonant peak and the frequency at which this peak occurs is known, simultaneous prediction of the amount of ammonia loading, whether empty or saturated, and the amount of soot loading at that instance is possible. It is a two-equation, two-variable problem. This can be used as a

reference map for all other cases and the sensor model can be calibrated inside the analyzer or control box to accurately predict the amount of soot and ammonia for light soot loading cases at every instance.

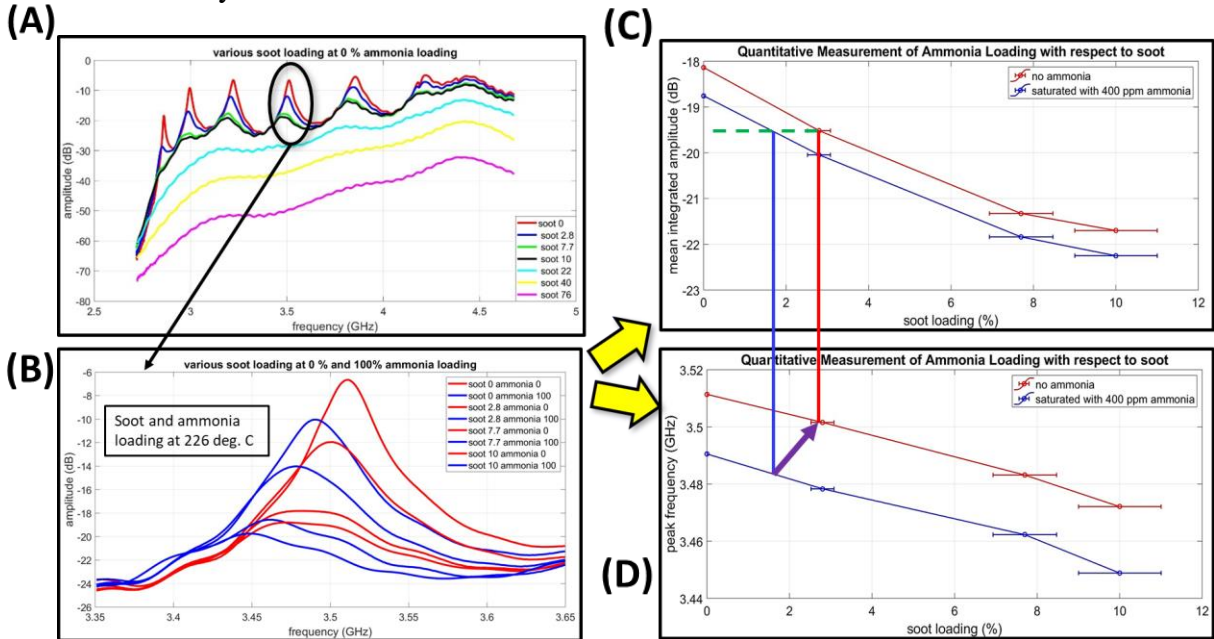


Figure 244: Quantitative analysis for simultaneously calculating soot and ammonia loading at light soot loading cases. (A) RF spectrum for all soot loading cases when no ammonia was stored in the SDPF. (B) 4th Resonant peak of the four light soot loading cases when no ammonia was stored in the SDPF. (B) 4th Resonant peak of the four light soot loading cases when the SDPF was empty and saturated with ammonia at the temperature of 226° C. (C) Mean amplitude of 4th Resonant peak in the frequency domain selected when SDPF was empty and saturated with ammonia. (D) peak frequency of the 4th resonant peak when the SDPF was empty and saturated of ammonia.

5 Conclusion

This experiment was conducted with an objective to analyze the RF and understand how the RF spectrum would change when conductivity and dielectric properties changes inside the SDPF due to the presence of soot and ammonia. The goal was to analyze the RF spectrum change in presence of soot loading and ammonia storage. Heavy-duty vehicles have ammonia injection or as generally called diesel exhaust fluid which is used to convert NO_x to N_2 and O_2 during the regeneration process. Keeping in mind the objectives, each test was run specifically to get appropriate results which gave the quantitative model of how the RF spectrum interacts with soot and ammonia, including temperature affects the spectrum. Finally, Correlatory quantitative models were designed, and analysis was carried out to report as quantitative results. Section two mentioned about the experimental setup. Each test in the experiment was ran in two phases first being preparation phase where soot was loaded in the SDPF and the second phase was testing phase where the entire test was run in a particular manner such that the RF spectrum could be recorded for stepwise increase in temperature from 100°C to 500°C in 100°C step increase. Then interaction of the RF spectrum and ammonia in presence of soot at a static temperature was analyzed before soot was burned away and ammonia desorbed. The temperature was then decreased stepwise similar to how it was increased to record spectrum for validation and verification that all the soot was burned away and ammonia desorbed before running the next test. Section 3 contained the results and observation, as soot loading was increased inside the SDPF the RF spectrum changes, the amplitude of resonant peaks decrease, the resonant peaks are formed at lower frequency and that they start getting less defined i.e. the constructive interference of electromagnetic waves happening inside the SDPF gets distorted hence, the resonant peaks are lost as soot loading is increased but, still the baseline spectrum was measured. The change in RF spectrum with stepwise increasing temperature was observed and it was concluded that in presence of soot loading, as the temperature is increased, baseline spectrum moves down i.e. decreases in intensity, but this decrease is dependent on the amount of soot loading. As soot loading is increased the change in the RF spectrum due to temperature variation also increases. The interaction of the RF spectrum with ammonia in the presence of soot was observed. From the results, it can be said that under light soot loading condition ammonia effect on RF spectrum in the presence of soot can be registered but as soot loading has increased this effect is negligible. Quantitative analysis for simultaneously calculating soot and ammonia loading at low loading case, to calculate the amount of soot present at various temperatures and show that in summation ammonia's effect can be neglected on the RF spectrum change under soot loading condition was conducted. The results and method for the same are highlighted in their sections. It can be said, after performing this experiment that RF spectrum changes with the amount of soot loading and ammonia effect on the RF spectrum can be neglected in the presence of soot. The quantitative model listed above was used to analyze the above-mentioned cases.

6 References

- [1] H. Nanjundaswamy, V. Nagaraju, Y. Wu, E. Koehler, A. Sappok, P. Ragaller, L. Bromberg, Advanced RF Particulate Filter Sensing and Controls for Efficient After-treatment Management and Reduced Fuel Consumption, SAE Technical Paper 2015-01-0996, 2015, doi:10.4271/2015-01-0996.
- [2] D. Rauch, D. Kubinski, U. Simon, R. Moos, Detection of the Ammonia Loading of a Cu Chabazite SCR Catalyst by a Radio Frequency-Based Method, *Sens. and Act. B: Chemical* 205 (2014) 88-93.
- [3] Sappok, A. and Bromberg, L., "Radio Frequency Diesel Particulate Filter Soot and Ash Level Sensors: Enabling Adaptive Controls for Heavy-Duty Diesel Applications," *SAE Int. J. Commer. Veh.* 7(2):2014, doi:10.4271/2014-01-2349.
- [4] Bromberg, L., Harris, T.M., Sappok, A., Guarino, A. et al., "Developing Design Guidelines for an SCR Assembly Equipped for RF Sensing of NH₃ Loading," SAE Technical Paper 2018-01-1266, 2018, doi:10.4271/2018-01-1266.
- [5] Sappok, Alex & Prikhodko, Vitaly & Parks, II & E, James. (2010). Loading and Regeneration Analysis of a Diesel Particulate Filter with a Radio Frequency-Based Sensor. SAE Tech. Pap.. 10.4271/2010-01-2126.
- [6] D. Rauch, D. Kubinski, G. Cavataio, D. Upadhyay, R. Moos, Ammonia loading detection of zeolite SCR catalysts using a radio frequency based method, *SAE Int. J Eng.* 8(3) (2015) 1126-1135.
- [7] M. Colombo, I. Nova, E. Tronconi, Detailed kinetic modeling of the NH₃-NO/NO₂SCR reactions over a commercial Cu-zeolite catalyst for diesel exhausts after-treatment, *Catal. Today* 197 (2012) 243–255.
- [8] U. Deka, A. Juhin, E.A. Eilertsen, H. Emerich, M.A. Green, S.T. Korhonen, B.M. Weckhuysen, A.M. Beale, Confirmation of isolated Cu²⁺ ions in SSZ-13 zeolite active sites in NH₃-selective catalytic reduction, *J. Phys. Chem. C* 116 (2012) 4809–4818.
- [9] R. Moos, D. Rauch¹, M. Votsmeier, D. Kubinski, Review on radio frequency based monitoring of SCR and three way catalysts, *Top. Catal.* 59 (2016) 961–969.
- [10] R.Q. Long, R.T. Yang, Reaction mechanism of selective catalytic reduction of NO with NH₃ over Fe-ZSM-5 catalyst, *J. Catal.* 207 (2002) 224–231.
- [11] U. Simon, U. Flesch, W. Maunz, R. Muller, C. Plog, The effect of NH₃ on the ionic conductivity of dehydrated zeolites Na beta and H beta, *Microporous and Mesoporous Materials* 21 (1998) 111–116.

- [12] Moos R (2010) Catalysts as sensors—a promising novel approach in automotive exhaust gas after-treatment. *Sensors* 10:6773–6787. doi:10.3390/s100706773
- [13] Moos R, Beulertz G, Reiß S, Hagen G, Fischerauer G, Votsmeier M, Gieshoff J (2013) Overview: status of the microwave-based automotive catalyst state diagnosis. *Top Catal* 56:483–488. doi:10.1007/s11244-013-9980-x
- [14] Beulertz G, Fritsch M, Fischerauer G, Herbst F, Gieshoff J, Votsmeier M, Hagen G, Moos R (2013) Microwave cavity perturbation as a tool for laboratory in situ measurement of the oxidation state of three way catalysts. *Top Catal* 56:405–409. doi:10.1007/s11244-013-9987-3
- [15] Moos R, Fischerauer G (2015) Automotive catalyst state diagnosis using microwaves. *Oil Gas Sci Technol* 70:55–65. doi:10.2516/ogst/2013203
- [16] Dietrich M, Jahn C, Lanzerath P, Moos R (2015) Microwave based oxidation state and soot loading determination on gasoline particulate filters with three-way catalyst coating for homogenously operated gasoline engines. *Sensors* 15:21971–21988. doi:10.3390/s150921971
- [17] Reiß S, Wedemann M, Spörrl M, Fischerauer G, Moos R (2011) Effects of H₂O, CO₂, CO, and flow rates on the RF-based monitoring of three-way catalysts. *Sensor Letters* 9:316–320. doi:10.1166/sl.2011.1472
- [18] Markus Dietrich, Gunter Hagen, Willibald Reitmeier, Katharina Burger, Markus Hien, Philippe Grass, David Kubinski, Jaco Visser and Ralf Moos. Radio-Frequency-Controlled Urea Dosing for NH₃-SCR Catalysts: NH₃ Storage Influence to Catalyst Performance under Transient Conditions. *Sensors* 2017, 17, 2746; doi:10.3390/s17122746
- [19] Ballinger, T., Cox, J., Konduru, M., De, D. et al., “Evaluation of SCR Catalyst Technology on Diesel Particulate Filters,” *SAE Int. J. Fuels Lubr.* 2(1):369-374, 2009, doi:10.4271/2009-01-0910.
- [20] Naseri, M., Chatterjee, S., Castagnola, M., Chen, H. et al., “Development of SCR on Diesel Particulate Filter System for Heavy Duty Applications,” *SAE Int. J. Engines* 4(1): 1798-1809, 2011, doi:10.4271/2011-01-1312.
- [21] J. Li, H. Chang, L. Ma, J. Hao, R.T. Yang, Low-temperature selective catalytic reduction of NO_x with NH₃ over metal oxide and zeolite catalysts—a review, *Catal. Today* 175 (2011) 147–156.
- [22] Paul J. Petersan and Steven M. Anlage, Measurement of resonant frequency and quality factor of microwave resonators: Comparison of methods, 1998 American Institute of Physics. [S0021-8979(98)04317-5]